Melatonin alleviates renal injury in diabetic rats by regulating autophagy

NA LUO[1,2*], YANGYANG WANG[3,4*], YONGGANG MA[3,4], YU LIU[1] and ZONGPING LIU[3,4]

[1]Department of Endocrinology, Sir Run Run Hospital, Nanjing Medical University, Nanjing, Jiangsu 211166; [2]Department of Endocrinology, Clinical Medical College, Yangzhou University, Northern Jiangsu People's Hospital, Yangzhou, Jiangsu 225001; [3]College of Veterinary Medicine; [4]Jiangsu Co-innovation Center for Prevention and Control of Important Animal Infectious Diseases and Zoonoses, Yangzhou University, Yangzhou, Jiangsu 225009, P.R. China

Received April 17, 2023; Accepted July 10, 2023

DOI: 10.3892/mmr.2023.13101

Abstract. Melatonin (MLT) is a biologically active indoleamine involved in regulating various biological rhythms, which is deficient in individuals with Type 2 diabetes. The present study examined the effects of MLT on diabetic neuropathy (DN). Diabetic rats received MLT treatment for 12 weeks, after which changes in kidney histology, oxidative damage, mitochondrial morphology and autophagy were measured. The glucose tolerance- and isoflurane tolerance-area under the curve (AUC) values and the relative renal weight index (RI) in the diabetes mellitus (DM) group of rats were significantly higher compared with those in the control group. A significant increase in malondialdehyde (MDA) content, and decreases in the activity of superoxide dismutase (SOD), catalase (CAT), glutathione peroxidase (GSH-Px) and GSH were demonstrated in the kidneys of DM rats compared with those in the control rats. Histological staining of DM rat kidney tissue with hematoxylin and eosin, Masson's trichome and Periodic acid-Schiff demonstrated glomerular and tubule lesions, and an increase in collagen compared with control rats. Protein expression levels of LC3II, P62, collagen IV (COL-IV) and α-SMA were increased in DM rats and HG-induced NRK-52E cells compared with those in the control groups. Phosphorylation of AMPK was reduced, whereas phosphorylation of PI3K, Akt and mTOR were increased *in vivo* and *in vitro*. Notably, MLT treatment significantly reduced glucose tolerance-AUC and RI, decreased MDA content, and increased SOD, CAT, GSH-Px and GSH activity. Glomerular and tubule lesions improved, collagen was decreased and mitochondrial damage was alleviated by MLT treatment. MLT treatment also decreased the protein expression levels of LC3II, P62 and COL-IV, whereas the phosphorylation of AMPK was significantly increased, which inhibited the phosphorylation of PI3K, AKT and mTOR *in vivo* and *in vitro*. These results demonstrated that MLT protects against DN and NRK-52E cell injury through inhibiting oxidative damage and regulating autophagy via the PI3K/AKT/mTOR signaling pathway.

Introduction

Diabetes mellitus (DM), one of the major risk factors for the initiation and progression of nephropathy, can cause kidney damage by inducing the production of reactive oxygen metabolites and attenuating antioxidative mechanisms (1). Diabetic nephropathy (DN) is characterized by both ultrastructural and morphological alternations in the kidney, including glomerular mesangial expansion, basement membrane thickening and tubular hypertrophy (2). The pathogenesis of DN is complex and oxidative stress is widely considered to contribute to its progression (3), as excessive reactive oxygen species (ROS) production, including mitochondrial ROS, causes oxidative stress, and can ultimately lead to mitochondrial damage and cellular death (4). Therefore, the effective prevention and treatment of DN is important.

An increasing body of evidence has suggested that autophagy is a potential therapeutic target for DN (5,6). Autophagy is an evolutionarily conserved biological process in cells that degrades damaged organelles and excess proteins to maintain normal balance in response to stress and injury (7). In this process, the unimpeded autophagic flux is important for autophagy to degrade organelles and proteins. Mitophagy is a selective type of autophagy, in which impaired mitochondria are degraded by lysosomes. However, dysfunction of autophagy

Correspondence to: Professor Yu Liu, Department of Endocrinology, Sir Run Run Hospital, Nanjing Medical University, 109 Long Mian Avenue, Nanjing, Jiangsu 211166, P.R. China
E-mail: drliuyu@njmu.edu.cn

Professor Zongping Liu, College of Veterinary Medicine, Yangzhou University, 48 Wenhui East Road, Hanjiang, Yangzhou, Jiangsu 225009, P.R. China
E-mail: liuzongping@yzu.edu.cn

*Contributed equally

Abbreviations: CAT, catalase; DN, diabetic nephropathy; DM, diabetes mellitus; GSH-Px, glutathione peroxidase; AUC, area under the curve; G-AUC, glucose tolerance-AUC; I-AUC, insulin tolerance-AUC; MLT, melatonin; MDA, malondialdehyde; SOD, superoxide dismutase

Key words: diabetes mellitus, melatonin, autophagy, kidney injury

can lead to certain diseases, including Alzheimer's disease (8), cardiovascular disease and inflammatory bowel disease (9). Cinacalcet-induced autophagy has previously been reported to protect against kidney damage in a DN model, acting through the CaMKKβ-LKB1-AMPK signaling pathway (10). In addition, overexpression of STAMP2 can attenuate renal injury by upregulating autophagy in DN (11). Lian *et al* (12) reported that inhibiting autophagy can aggravate lead-induced kidney injury. These previous studies suggested that autophagy serves an important role in DN.

Melatonin (MLT; 5-methoxy-*N*-acetyltryptamine) is secreted by the pineal gland and is a natural antioxidant that inhibits oxidative stress by scavenging ROS (13). Once synthesized, MLT binds to two specific G protein-coupled receptors: MLT receptor type 1 (MTI) and MLT receptor type 2 (MT2) (14). In diabetic kidney injury, MLT can mediate the anti-apoptotic effect of MT2 and can also regulate mitochondrial fission/fusion homeostasis, leading to protective effects (15,16). In addition, MLT activates Wnt/β-catenin and TGF-β1-Smad2/3 signaling pathways to alleviate oxidative stress, which inhibits TLR4 or NF-κB and TGF-β1/Smad3 signaling pathways to improve renal inflammation and fibrosis (17-19). It has also been reported that MLT serves an essential role in anti-inflammatory processes, such as rheumatoid arthritis (20,21). Yu *et al* (22) and Zhang *et al* (23) previously reported that MLT can augment mitochondrial function via modulating AMPK activity and autophagy. Siddhi *et al* (24) also reported that MLT prevents DN by modulating the AMPK/SIRT1 signal pathway via recovering the autophagy and mitochondrial function. In addition, Qiu *et al* (25) reported that MLT suppresses ferroptosis via activation of the Nrf2/HO-1 signaling pathway in a mouse model of sepsis-induced acute kidney injury. Therefore, the protective mechanisms underlying the effects of MLT on DM-induced kidney injury involve glucose homeostasis, oxidative stress, inflammation and apoptosis. However, the pathogenesis of DM-induced kidney injury is complex, and the mechanisms underlying the protective effects of MLT against this disease are not yet fully understood.

In the present study, the effects of MLT treatment on fibrosis, oxidative damage and autophagy levels in the kidneys of rats with DM were assessed.

Materials and methods

Experimental animal model. A total of 30 healthy clean-grade male 6-week-old Sprague-Dawley (SD) rats (weight, 80±15 g) were purchased from Liaoning Changsheng Biotechnology [animal license no. SCXK (Liao) 2020-0001]. The experimental procedures were approved by the Ethics Committee of Yangzhou University [Yangzhou, China; approval no. SYXK (Su) 2022-0044]. High-sugar and high-fat feed was purchased from Jiangsu Synergy Pharmaceutical & Biological Engineering Co., Ltd. Rats were maintained in a specific-pathogen-free housing facility at a constant temperature of 25˚C and 40-70% humidity under a 12-h dark/light cycle, with free access to water and standard clean-grade foods, and were acclimated for 1 week before being fed high-sugar and high-fat feed for 4 weeks. A total of 20 rats were randomly divided into control and modeling groups after being fed a high-fat, high-sugar diet for 5 weeks. The modeling group was intraperitoneally injected with 35 mg/kg streptozotocin [STZ; dissolved in 0.01 mol/l citrate buffer (pH 4.3)] after 12 h of fasting without water to produce the DM rat model. The control group of rats was intraperitoneally injected with an equal volume of PBS. Fasting blood glucose (FBG) was measured using small drops of blood collected from the tail for 3 consecutive days. Rats with a stable FBG ≥16.7 mmol/l were considered a successful model of DM. The total duration of the experiment was 17 weeks.

The health and behavior of rats were monitored daily and no animals died prior to sacrifice. All rats were sacrificed by cervical dislocation and death was verified by the cessation of respiratory movements. Diethyl ether was used for anesthesia prior to sacrifice. This method was approved by the Ethics Committee of Yangzhou University [approval no. (SYXK (Su) 2022-0044)]. Briefly, animals were placed in a plexiglass anesthesia box and a beaker containing a cotton ball of diethyl ether was placed inside the box. Respiratory rate was monitored to ensure that the animals were fully anesthetized. For blood glucose (BG) detection, small drops of blood were obtained from the tail using a lancet; the blood was then placed onto BG test strips, which were placed into a BG meter to obtain the BG value.

Detection of lipid metabolism. Blood lipids were detected using an automatic biochemical analyzer (AU5800; Beckman Coulter, Inc.).

Serum preparation. Blood samples of rats were taken from the heart and centrifuged at 1,000 x g at 4˚C for 15 min. Serum was collected and filtered through a 0.22-μm filter and stored at -80˚C until use.

Cell culture. The NRK-52E cell line was purchased from MilliporeSigma. Cells were cultured in DMEM (Gibco; Thermo Fisher Scientific, Inc.) supplemented with 10% fetal bovine serum (Gibco; Thermo Fisher Scientific, Inc.) at 37˚C in a humidified 5% CO_2 atmosphere. Cells were treated with 30 mM glucose and 60 μM MLT at 37˚C for 24 h.

Experimental groupings. The *in vivo* portion of the present study was divided into three experimental groups: i) Control; ii) DM group; and iii) DM + MLT group (n=10 per group). The concentration of 10 mg/l MLT in water was freely available every night. The *in vitro* portion of the present study was also divided into three experimental groups: i) Control; ii) high glucose (HG) group; and iii) HG + MLT (60 μM) group.

Cell transfection. The plasmids were obtained from Professor Lin Wang (Shandong Agricultural University, College of Veterinary Medicine, Taian, Shangdong, China). After treatment with glucose and MLT, and once NRK-52E cells reached 60-70% confluence, the RFP-GFP-LC3 plasmid was transfected into cells using Lipofectamine® 2000 transfection reagent (Invitrogen; Thermo Fisher Scientific, Inc.) for the detection of autophagic flux. 200 μl transfection system with 1 μg plasmid at 37˚C for 24 h. The time interval between transfection and subsequent experimentation was 24 h. Subsequently the cells were treated with glucose and MLT. In the present study, every

group of cells was transiently transfected; therefore, there were no negative or positive transfection controls. When the autophagosome and lysosome did not fuse, both RFP and GFP fluorescence were observed; however, when the autophagosome and lysosome fused, resulting in GFP quenching, only RFP fluorescence could be observed.

Reagents. The following reagents and materials were purchased for use in the present study: STZ (MilliporeSigma); MLT (purity >98%; MilliporeSigma); anhydrous glucose (Macklin, Inc.); insulin (Novo Nordisk A/S); BG meter and test strips (Roche Diagnostics); β-actin (cat. no. 93473SF) antibodies (Cell Signaling Technology, Inc.); anti-collagen IV (COL-IV; cat. no. AF0510) antibodies (Affinity Biosciences); anti-LC3 (cat. no. 4599T) antibodies (Cell Signaling Technology, Inc.); anti-P62 (cat. no. 23214S) antibodies (Cell Signaling Technology, Inc.); ECL Chemiluminescence Kit and BCA Protein Concentration Assay Kit (Beyotime Institute of Biotechnology); and malondialdehyde (MDA, cat. no. A003-1-2), superoxide dismutase (SOD, A001-3-2), catalase (CAT, A007-1-1), glutathione peroxidase (GSH-Px, A005-1-2) and GSH (A006-2-1) ELISA assay kits (Nanjing Jiancheng Bioengineering Institute).

Oral glucose tolerance test (OGTT) and intraperitoneal insulin tolerance test (IPITT). OGTT was performed 1 week prior to euthanasia. Animals were fasted for 12 h and were then orally administered 50% glucose solution (2 g/kg). BG levels were determined from tail blood samples at 0, 30, 60, 90 and 120 min. IPITT was performed 1 week prior to euthanasia. Animals were fasted for 4 h, after which, 1.5 U/kg insulin was injected intraperitoneally. BG was measured from tail blood samples at 0, 30, 60, 90 and 120 min. As aforementioned, BG was detected from small drops of blood collected from the tail using a lancet; the blood was then placed onto BG test strips, which were placed into a BG meter to obtain the BG value. The area under the curve (AUC) was calculated as follows=[0.5 x (BG at 0 min + BG at 30 min)/2] + [0.5 x (BG at 30 min + BG at 60 min)/2] + [1 x (BG at 60 min + BG at 120 min)/2].

Renal tissue oxidative damage index test. Renal tissue was collected in 1.5 ml centrifuge tube.

To prepare 10% tissue homogenate, kidney tissues were placed in saline and centrifuged at 1,000 x g for 10 min at 4˚C. The supernatant was collected to evaluate MDA, GSH-Px and GSH levels and SOD and CAT activity levels by ELISA kits according to manufacturer's protocols. Protein concentrations were measured using a BCA assay. All results were normalized to protein concentrations and expressed as U/mg protein or nmol/mg protein, as appropriate.

Hematoxylin and eosin (H&E), Masson's trichome and Periodic acid-Schiff (PAS) staining. Right kidney cortical tissues were fixed with 4% formalin to prepare tissue sections at room temperature for 24 h and the tissues embedded in paraffin. Sections (1x1x1 cm) were dewaxed and stained with H&E (1% hematoxylin was stained for 5 min, dye with 0.5% eosin solution for 1-3 min), Masson's trichome (Masson Ponceau acidic complexing liquid: Ponceau 0.7 g, acidic complexing 0.3 g, distilled water 99 ml, glacial acetic acid 1 ml, for 5-10 min) and PAS staining for 10 min at room temperature. The morphological changes of kidney tissues in each group were observed using a light microscope (Nikon Corporation).

Transmission electron microscopy (TEM). Fresh kidney tissues were cut into tissue blocks ~1x1x1 mm and were fixed with 2.5% glutaraldehyde at 4˚C overnight. Subsequently, the tissues were rinsed with PBS. NRK-52E cells were collected in a 1.5-ml centrifuge tube and fixed with 2.5% glutaraldehyde at 4˚C for 24 h. Samples were dehydrated using an ethanol gradient (45-95%), soaked and embedded in epoxy resin overnight at room temperature, then ultra-thin sections (<100 nm) were cut. Uranium acetate was placed on the wax plate or on the soaked filter paper, the carrier mesh with the sections placed in the dye solution (cut side in contact with the stain) for 15-30 min, the sections were rinsed with double distilled water, blotted with filter paper, and then the carrier mesh covered with 30 g/l lead citrate stain (to prevent the formation of lead carbonate precipitation, solid sodium hydroxide was placed in the petri dish). After staining for 5-10 min, the sections were rinsed with double steaming water, blotted dry, placed in a clean petri dish for later use and imaged using TEM (Philips Healthcare).

Immunohistochemistry and immunofluorescence. The kidney tissue embedded in paraffin wax was sectioned at ~5 μm thick. After the paraffin sections were dewaxed, the sections were washed with clean water after dewaxing solution I (10 min), Dewaxing solution II (10 min), Dewaxing solution III (10 min), anhydrous ethanol I (5 min), anhydrous ethanol II (5 min) and anhydrous ethanol III (5 min) in sequence. For antigen retrieval (EDTA pH 9.0) was added to a microwaveable vessel into which the slides were placed. The vessel was placed inside the 1,200 W microwave. The EDTA was boiled for 8 min at 1,200 W, then under medium heat before a pause for 8 min, followed by low and medium heat for 7 min. Following heat recovery of antigens, endogenous peroxidase activity was blocked using 0.3% hydrogen peroxide for 10 min at room temperature. After preincubation with 10% BSA (MilliporeSigma) for 10 min at room temperature to prevent nonspecific binding of antibodies, renal tissues were incubated with primary antibodies against COL-IV (1:500) overnight at 4˚C. After incubation with the appropriate secondary antibodies, sections were developed with 3,3'-diaminobenzidine and then counterstained with hematoxylin for 5 min (all at room temperature). Images were captured using a fluorescence microscope (Leica Microsystems GmbH).

Kidney tissues were sectioned, dewaxed, rehydrated and subjected to microwave antigen recovery in citrate buffer for 15 min as aforementioned in immunohistochemistry. After cooling, slides were blocked with 4% hydrogen peroxide for 10 min at room temperature, 5% BSA (MilliporeSigma) for 1 h at room temperature, then incubated with primary antibodies LC3 (cat. no. 4599T) and P62 (cat. no. 23214S), both at 1:100 overnight at 4˚C. Slides were washed with PBS and incubated with secondary antibodies (FITC-labeled mouse IgG; cat. no. A0568, Beyotime Institute of Biotechnology; 1:500) for 1 h at room temperature. Slides were washed and stained with DAPI at room temperature for 3 min to visualize the nuclei

and images were captured using a fluorescence microscope (Leica Microsystems GmbH).

NRK-52E cells were transfected with the RFP-GFP-LC3 plasmid, then fixed with 4% paraformaldehyde for 15 min at room temperature. Cells were imaged using a confocal microscope.

Western blotting. Kidney tissues and NRK-52E cells were homogenized in RIPA (NCM Biotech) buffer containing a protease inhibitor mixture (cat. no. P001; NCM Biotech) and centrifuged at 13,000 x g at 4˚C for 10 min. The supernatant was collected and protein concentrations were quantified using the BCA assay. Protein concentration was made uniform with the addition of lysate, 5X SDS Loading Buffer was added to samples by volume and mixed, and the samples were boiled at 100˚C for 10 min. Equivalent amounts of protein (30 μg) were separated by SDS-PAGE on 8-12% gels and transferred to polyvinylidene difluoride membranes with transfer buffer at room temperature for 1.5 h. Membranes were then blocked in 5% skim milk powder dissolved in TBST (20% Tween) for 2 h at room temperature. The following target antibodies were then added to the membranes: LC3 (cat. no. 4108S; 1:1,000; Cell Signaling Technology, Inc.), P62 (cat. no. P0067; 1:1,000, MilliporeSigma) and COL-IV (cat. no. AF0510; 1:1,000, Affinity Biosciences), α-SMA (cat. no. 19245T; 1:1,000; CST), ATG5 (cat. no. 12994T; 1:1,000; CST), ATG7 (cat. no. 8558T; 1:1,000; CST), TGF-1β (cat. no. 3709S; 1:1,000; SCT), AMPK (cat. no. 4150T; 1:1,000; CST), P-AMPK (cat. no. 50081S, 1:1,000, CST), PI3K (cat. no. 4249T, 1:1,000, CST), phosphorylated (p-)PI3K (cat. no. 17366, 1:1,000, CST), AKT (cat. no. 4691, 1:1,000, CST), p-AKT (cat. no. 4060, 1:1,000, CST), m-TOR (cat. no. 2983; 1:1,000; CST), p-mTOR (cat. no. 5536T; 1:1,000; CST), MT1 (cat. no. sc-390328; 1:500; Santa Cruz Biotechnology, Inc), MT2 (cat. no. c-398788; 1:500; Santa Cruz Biotechnology, Inc.) and β-actin (cat. no. 4970T; 1:1,000; CST). The secondary antibody (cat. no. 7074P2; 1:5,000; CST) was incubated for 2 h at room temperature. Protein bands were visualized using a chemiluminescence kit (NCM Biotech). Semi-quantification of protein expression levels was performed using ImageJ 8.0 software (National Institutes of Health).

Statistical analysis. SPSS software (version 26; IBM Corp.) was used for data analysis. One-way ANOVA followed by Tukey's or Tamhane's test, or unpaired Student's t-test, were used to determine statistical significance between groups. Data are expressed as the mean ± standard deviation. Each experiment was repeated three times. $P<0.05$ was considered to indicate a statistically significant difference.

Results

Effects of MLT on glucose and insulin tolerance, renal weight index (RI), lipid metabolism and oxidative damage in diabetic rats. The potential protective effects of MLT against DN in a rat model of DM were examined (Fig. 1A). To evaluate glucose and insulin tolerance, BG levels were measured at different time points (0, 30, 60, 90 and 120 min) following treatment with glucose and insulin in DM rats, As shown in Fig. 1B, the glucose tolerance-AUC (G-AUC) and insulin tolerance-AUC (I-AUC) values were significantly higher in rats in the DM group compared with those in the control group. After treatment with MLT, G-AUC was significantly lower in rats compared with that in the DM group, whereas I-AUC was not significantly different in MLT-treated rats compared with that in DM rats. Serum creatinine and urine albumin-creatinine ratio levels were significantly increased in the DM group compared with those in the control group, whereas MLT treatment significantly decreased these levels compared with those in the DM group. The relative RI was calculated as follows: Kidney weight/body weight. The relative RI of DM rats was significantly increased compared with that in the control group, whereas MLT treatment inhibited the increase in relative RI. Therefore, these results suggested that MLT improved glucose tolerance in DM rats but had no significant effect on insulin tolerance.

The effects of MLT on lipid metabolism were also examined. Compared with those in the control group, the DM group of rats demonstrated significantly increased total cholesterol (TC), triglycerides (TG) and low-density lipoprotein (LDL) levels (Fig. 1C). After 12 weeks of MLT treatment, TC, TG and LDL levels were significantly decreased compared with those in the DM group. However, compared with those in the control group, high-density lipoprotein (HDL) levels were reduced in the DM group and after treatment with MLT, HDL levels were significantly increased compared with those in the DM group (Fig. 1D). These results suggested that MLT treatment partially recovered the lipid metabolism levels in diabetic rats.

The effects of MLT on oxidative damage were also examined. Compared with in the control group, the DM group of rats demonstrated a significant increase in MDA content, and a significant decrease in SOD, CAT, GSH-PX and GSH activities (Fig. 1D). After intervention with MLT, MDA content was significantly lower, and levels of SOD, CAT, GSH-PX and GSH were significantly higher compared with those in the DM group. These data suggested that MLT significantly reduced oxidative damage in DM rats.

Effects of MLT on histopathological changes in kidney tissue in DM rats. The effects of MLT treatment on histopathological changes in the kidneys of DM rats were evaluated. H&E staining demonstrated that the DM group exhibited thickening of the glomerular basement membrane and shrinkage of the glomeruli (red arrow). In addition, some tubular epithelial cells were vacuolated, necrotic, atrophied and detached, and infiltration of interstitial inflammatory cells was observed (yellow arrow; Fig. 2). However, in the control group, the renal tubule structure was clearly visible, epithelial cells were neatly arranged, the basement membrane was more intact and there was no major collagen fiber deposition. PAS staining further demonstrated that the glomerular basement membrane in DM rats was thickened (red arrow). Masson's trichome staining demonstrated blue collagen fiber deposition in the interstitial glomeruli and tubules of DM rats (red arrow). Following intervention with MLT, glomerular and tubular lesions, interstitial inflammatory cell infiltration, congestion and collagen fiber deposition were reduced. These results suggested that MLT protected against kidney injury.

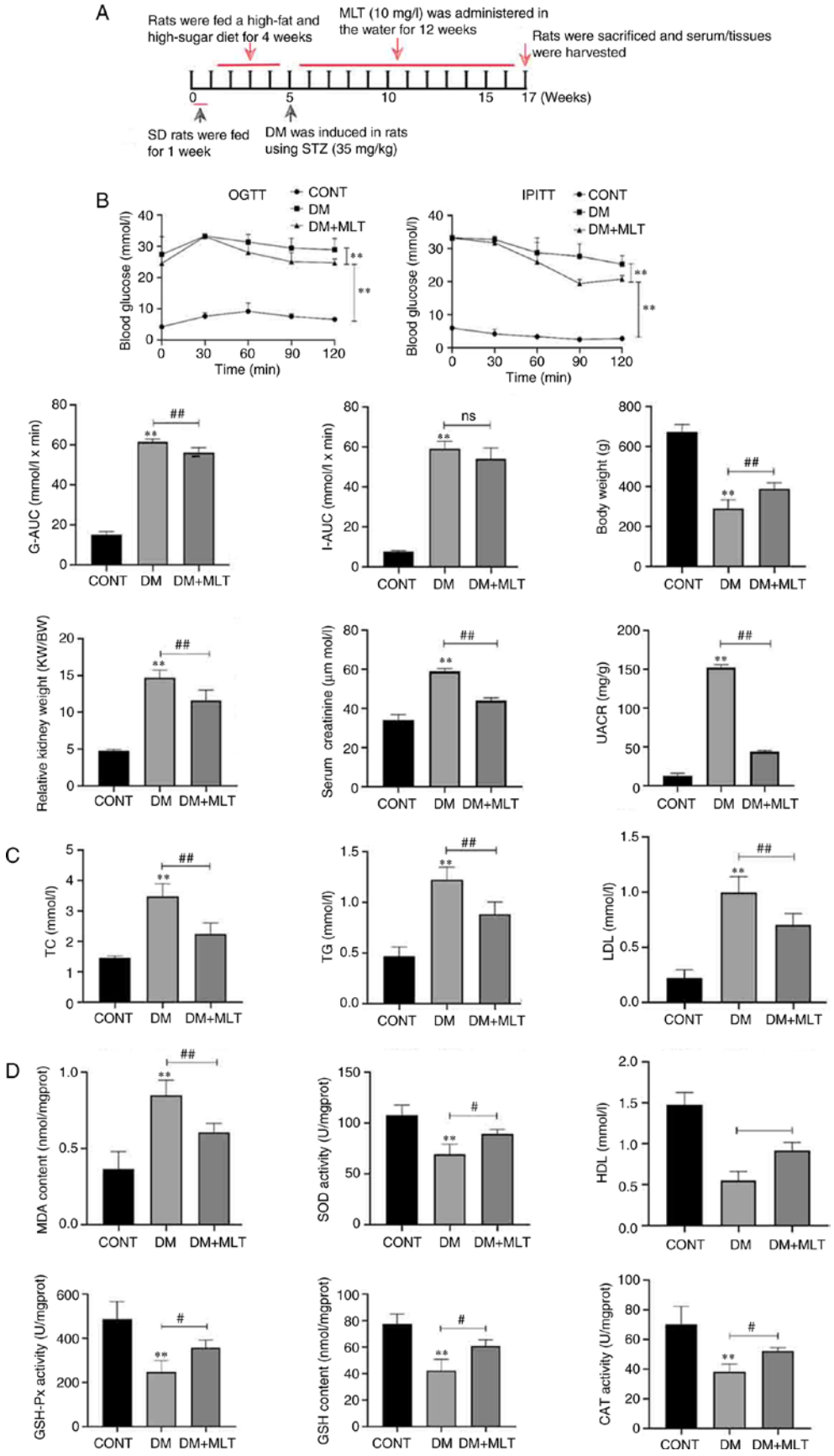

Figure 1. Effects of MLT on glucose tolerance, insulin tolerance, relative renal weight index, lipid metabolism and oxidative damage in DM rats. (A) Treatment protocol to evaluate potential protective effects of MLT in DM rats. (B) G-AUC, I-AUC and relative renal weight index of rats in each group. OGTT, IPITT, serum creatinine and UACR levels were analyzed. (C and D) ELISA kits were used to measure kidney injury index. Data are presented as the mean ± standard deviation (n=5). **P<0.01 vs. CONT; $^{\#}$P<0.05 $^{\#\#}$P<0.01 vs. DM, Sprague Dawley; DM, diabetes mellitus; STZ, streptozotocin; CONT, control; MLT, melatonin; OGTT, oral glucose tolerance test; IPITT, intraperitoneal insulin tolerance test; G-AUC, glucose tolerance-area under the curve; I-AUC, insulin tolerance-area under the curve; UACR, urine albumin-creatinine ratio; TC, total cholesterol; TG, triglycerides; LDL, low-density lipoprotein; MDA, malondialdehyde; SOD, superoxide dismutase; HDL, high-density lipoprotein; GSH-Px, glutathione peroxidase; CAT, catalase; ns, not significant; KW, kidney weight; BW, body weight.

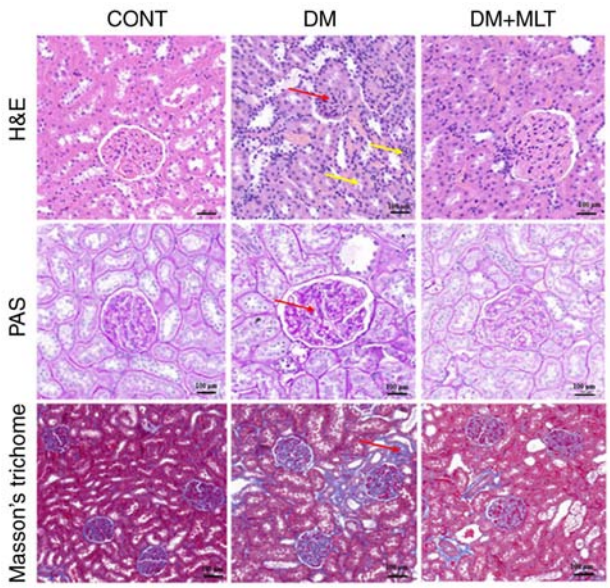

Figure 2. Effects of MLT on the histopathology of kidney tissue in DM rats. Renal tissues of rats in each group were stained with H&E, PAS and Masson's trichome. Scale bar, 100 μm. CONT, control; DM, diabetes mellitus; MLT, melatonin; H&E, hematoxylin and eosin; PAS, Periodic acid-Schiff.

Effects of MLT on renal fibrosis and MLT receptors. The expression levels of COL-IV in kidney tissue were examined and it was demonstrated that the protein expression levels of COL-IV were markedly increased in the kidney tissue of DM rats compared with those in the control rats (Fig. 3A). MLT reduced the protein expression levels of COL-IV compared with those in the DM group. In NRK-52E cells, HG treatment caused an increase in the protein expression levels expression of α-SMA, COL-IV and TGF-β1 compared with those in the control group (Fig. 3B). MLT treatment markedly reduced the expression levels of these proteins.

The effects of MLT were also assessed on the expression of MT1 and MT2 in both kidney tissue and NRK-52E cells. No marked change was demonstrated in MT1 and MT2 expression in DM rats compared with that in the control group. Following treatment with MLT, the expression levels of MT1 and MT2 were significantly increased compared with those in the DM group (Fig. 3C and D). In NRK-52E cells, HG induced cellular injury (red arrows); however, after treatment with MLT, cell injury was reduced (Fig. 3E). Next, the effect of MLT on MT1 and MT2 expression levels in NRK-52E cells was examined (Fig. 3F). MLT treatment increased the expression levels of MT1 and MT2 in HG-induced NRK-52E cells compared with those in the HG group. These results suggested that MLT exerts a protective effect against DM-induced kidney damage and HG-induced NRK-52E cell injury.

Effects of MLT on mitochondrial structure and autophagy in kidney tissue of DM rats and NRK-52E cells. TEM was used to examine the structure of mitochondria and autophagosomes in DM rat kidney tissue. Compared with those in the control group, the mitochondria of kidney cells in the DM group were dilated and swollen, cristae were reduced or absent (yellow arrow) and a large number of mitochondria were surrounded by a double-membrane structure (red arrow), forming autophagosomes (Fig. 4A). After treatment with MLT for 12 weeks, a reduction in mitochondrial damage in rat kidney tissues was observed, in addition to a reduction in the number of damaged mitochondria wrapped in bilayer membranes. Immunofluorescence was used to measure the expression of LC3 and P62 in DM rat kidney tissue. Compared with that in the control group, the fluorescence intensity of LC3 and P62 were increased in the DM group (Fig. 4B). MLT treatment reduced the fluorescence intensity of LC3 and P62 compared with that in the DM group. Immunohistochemistry was used to analyze the expression levels of autophagy protein (ATG)5, ATG7 and LC3. The expression levels of ATG5, ATG7 and LC3 were increased in the kidneys of DM rats compared with those in the control rats and MLT treatment reduced the expression levels of these proteins (Fig. 4C). Western blotting was used to semi-quantify the protein expression levels of autophagy-related proteins. In DM rats, the protein expression levels of ATG5, ATG7, P62 and LC3II/I were significantly increased, whereas MLT treatment significantly reduced the expression of these proteins (Fig. 4D).

To further examine the effect of MLT on DM-induced autophagy, NRK-52E cell model was induced by HG. TEM was used to detect the mitochondrial structure in HG-induced NRK-52E cells and demonstrated that the mitochondrial ridge disappeared, mitochondria were swollen (yellow arrow) and numerous mitophagosomes (red arrow) were observed (Fig. 4E). After MLT treatment, mitochondrial structures were generally intact and mitophagosome numbers were reduced. To determine the mechanism by which this occurs, western blotting and immunofluorescence were used to analyze changes in autophagy. HG inhibited autophagy degradation by mediating an increase in the protein expression levels of P62, whereas MLT treatment reduced the protein expression levels of P62 and LC3II and decreased the yellow fluorescence signal (Fig. 4F and G). Therefore, these data suggested that MLT protected mitochondria structure in DM rat tissues and HG-induced NRK-52E cells and could also regulate autophagy levels.

Effects of MLT on AMPKα/PI3K/AKT/mTOR signaling in DM rats and NRK-52E cells. To further examine the effect of MLT on the regulation of the autophagy pathway, western blotting was used to examine the expression of autophagy-related signaling pathway proteins. In DM rat kidney tissues and NRK-52E cells, the phosphorylation levels of the key autophagy protein AMPKα were significantly decreased, whereas the phosphorylation levels of PI3K, AKT and mTOR were significantly increased compared with those in the control groups (Fig. 5A and B). After treatment with MLT, the phosphorylation levels of AMPKα were significantly increased, whereas the phosphorylation levels of PI3K, AKT and mTOR were significantly decreased. These results suggested that MLT affected the AMPKα/PI3K/AKT/mTOR signaling pathway, which is important for autophagy formation.

Discussion

Diabetes mellitus (DM) is one of the chronic metabolic noncommunicable diseases that has become a worldwide epidemic (26). DN is one of the most common microvascular

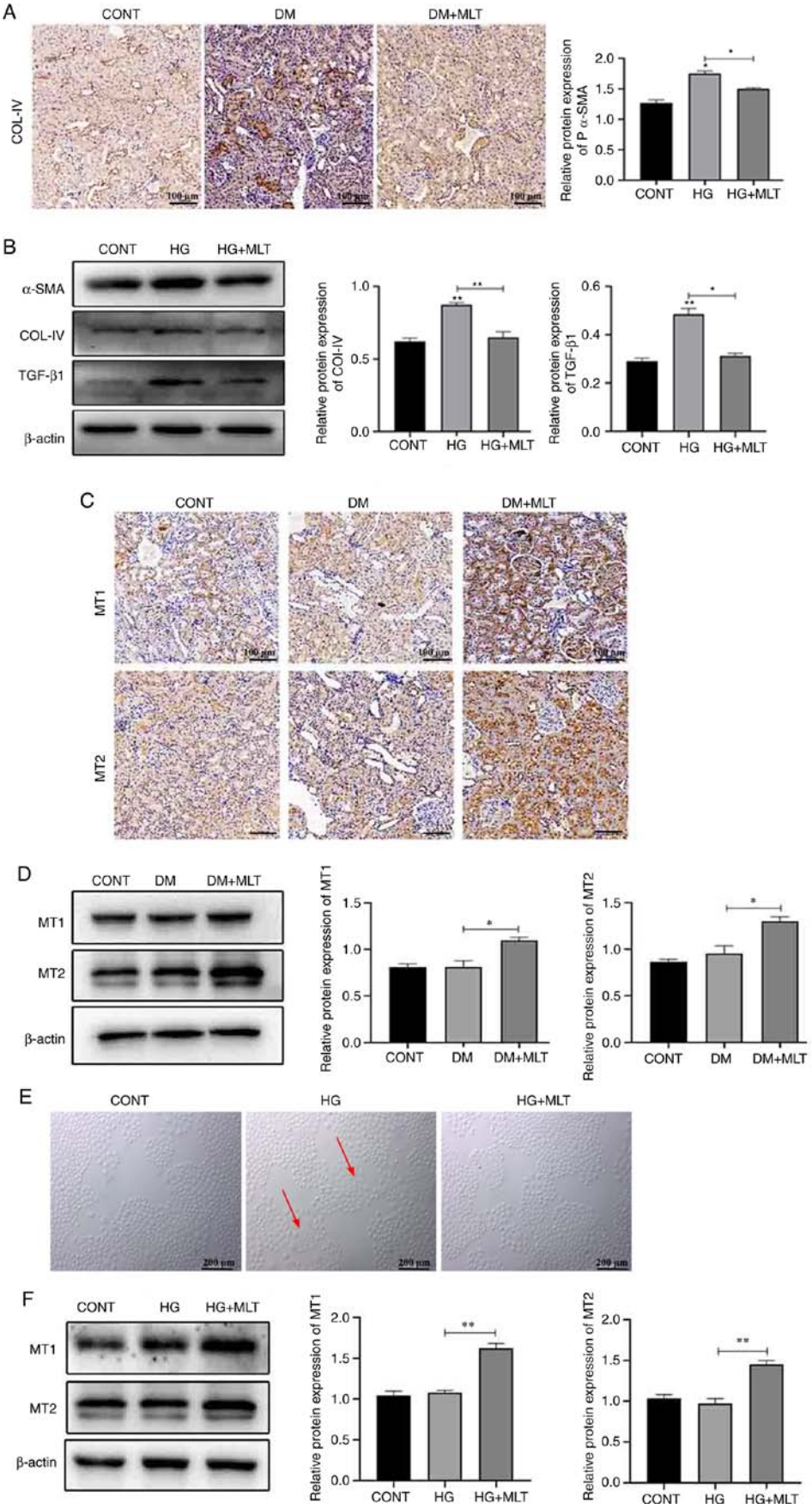

Figure 3. Effects of MLT on renal fibrosis and MLT receptors. (A) Immunohistochemical staining of COL-IV in kidney tissue of DM rats. Scale bar, 100 μm. (B) Protein expression levels of α-SMA, COL-IV, TGF-β1 and β-actin in HG- and MLT-treated cells. (C) Immunohistochemical staining of MT1 and MT2 in kidney tissue of DM rats. (D) Protein expression levels of MT1 and MT2 in kidney tissue of DM rats treated with MLT. (E) Morphological changes of NRK-52E cells with HG and MLT treatment (red arrows indicate damaged cells). Scale bar, 200 μm. (F) Protein expression levels of MT1 and MT2 in NRK-52E cells treated with HG and MLT. Data are presented as the mean ± standard deviation (n=3). *P<0.05, **P<0.01. CONT, control; DM, diabetes mellitus; MLT, melatonin; COL-IV, type IV collagen; HG, high glucose; MT1, melatonin receptor 1; MT2, melatonin receptor 2.

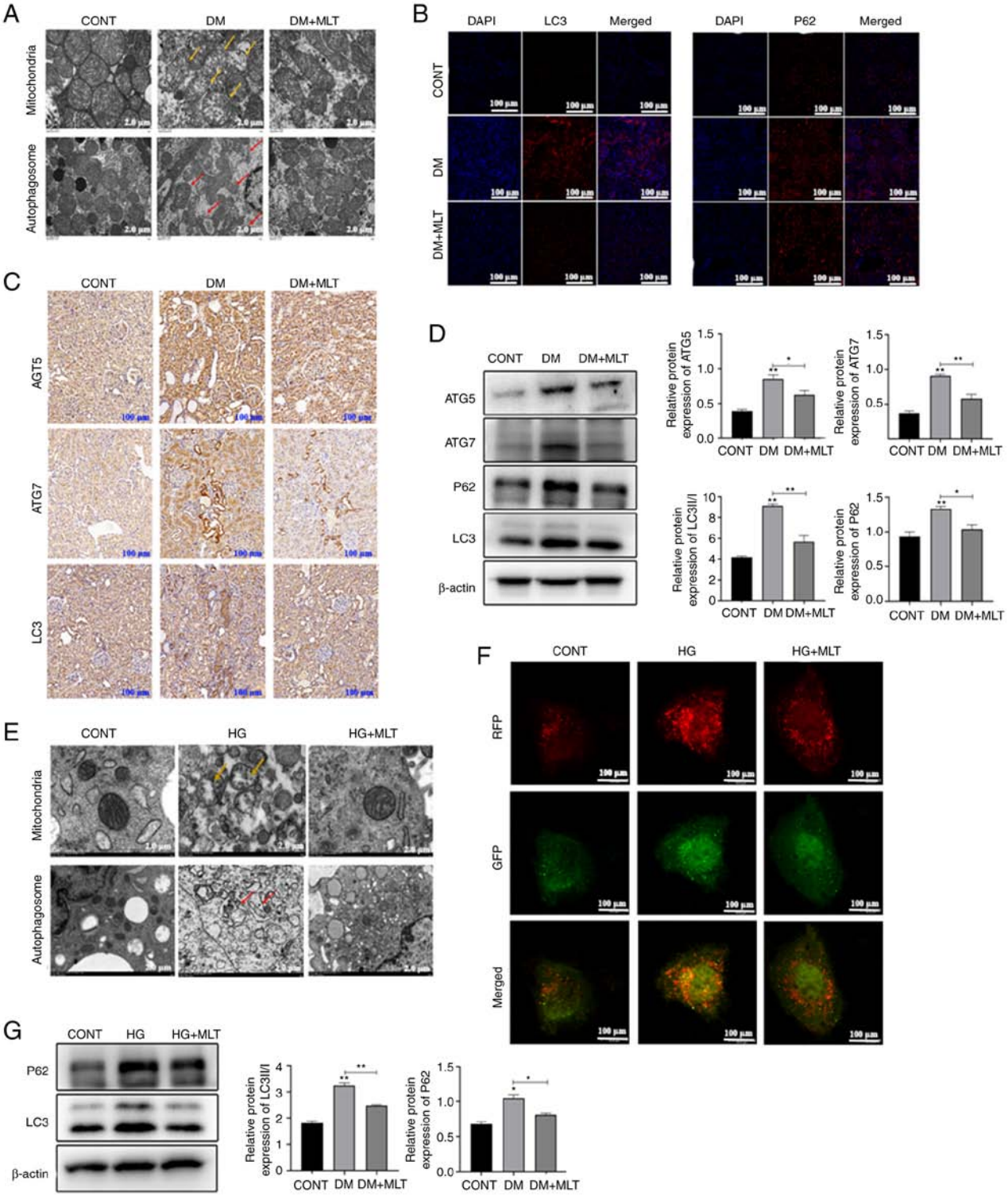

Figure 4. Effects of MLT on mitochondria structure and autophagy in kidney tissue of DM rats and NRK-52E cells. (A) Ultrastructure of mitochondria and autophagosomes of kidney cells of DM rats treated with MLT (yellow arrow indicates damaged mitochondria; red arrow indicates autophagosomes). Scale bar, 2 μm. (B) LC3 and P62 immunofluorescence staining of kidney tissues of DM rats treated with MLT. Scale bar, 100 μm. (C) Immunohistochemical staining of ATG5, ATG7 and LC3 in kidneys of DM rats treated with MLT. Scale bar, 100 μm. (D) Protein expression levels of ATG5, ATG7, P62, LC3 and β-actin in kidney tissue of DM rats. (E) Ultrastructure of mitochondria and autophagosomes of NRK-52E cells treated with HG and MLT (yellow arrow represents indicates mitochondria; red arrow indicates autophagosomes). Scale bar, 2 μm. (F) RFP and GFP immunofluorescence staining of NRK-52E cells treated with HG and MLT. Scale bar, 100 μm. (G) Protein expression levels of P62, LC3 and β-actin in NRK-52E cells treated with HG and MLT. Data are presented as the mean ± standard deviation (n=3). *P<0.05, **P<0.01. CONT, control; DM, diabetes mellitus; MLT, melatonin; HG, high glucose; ATG, autophagy-related protein.

complications associated with DM and is a major cause of end-stage renal disease (ESRD) (27). The onset of DM causes certain pathological changes in kidneys, including the deposition of extracellular matrix mainly in the glomerular membrane, thickening of the glomerular basement membrane, proliferative changes and tubular atrophy, ultimately leading to

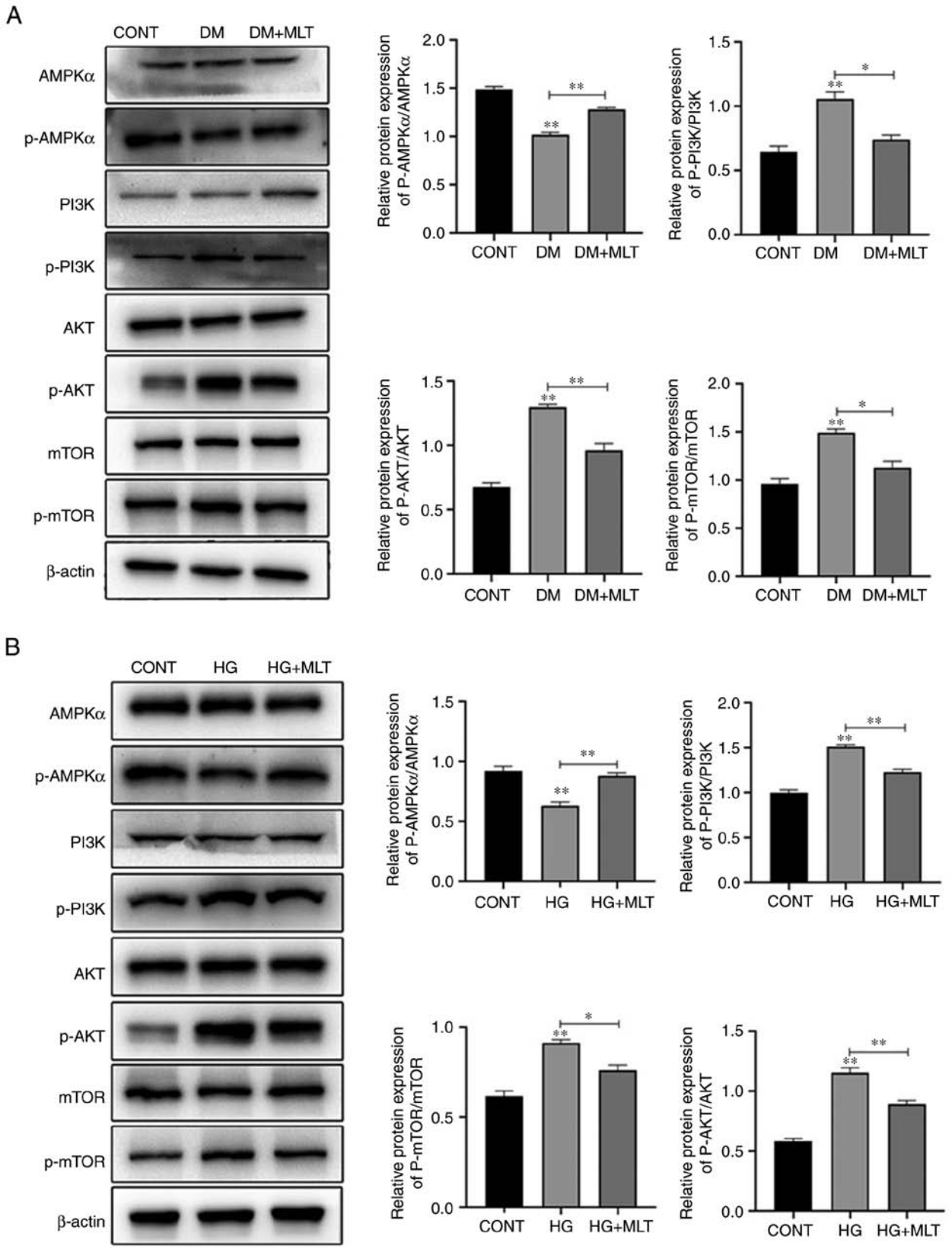

Figure 5. Effects of MLT on protein expression and phosphorylation levels of AMPKα, PI3K, AKT and mTOR signaling in (A) kidney tissue of DM rats treated with MLT and (B) NRK-52E cells treated with HG and MLT. Data are presented as the mean ± standard deviation (n=3). *P<0.05, **P<0.01. CONT, control; DM, diabetes mellitus; MLT, melatonin; HG, high glucose; P, phosphorylated.

interstitial fibrosis and glomerulosclerosis (28). In the present study, the aforementioned features of kidney tissue damage were demonstrated in rats with DM, such as mitochondrial expansion and swelling, and reduction or disappearance of cristae, indicating that DM rats were a suitable model for DN. In addition, hyperglycemia also increases ROS production,

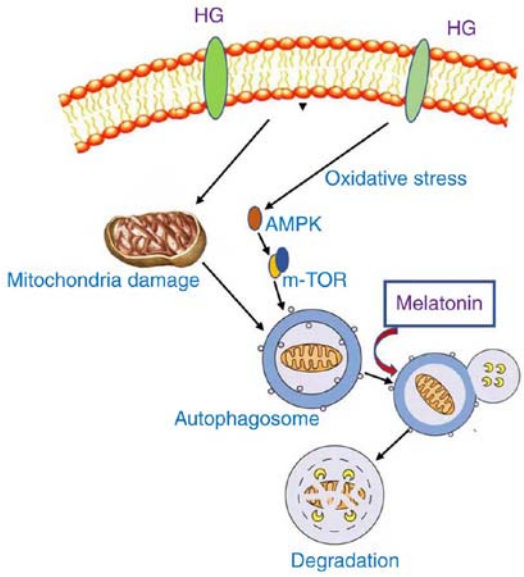

Figure 6. Mechanism of melatonin-induced regulation of autophagy. HG, high glucose.

and excessive ROS can lead to increased expression of extracellular matrix genes by regulating the activation of PKC, mitogen-activated protein kinase and certain cytokines (IL-18) and transcription factors (NF-κB), which can lead to the development of fibrosis and ESRD (29).

In the present study, the MDA content in DM rat kidney tissues was significantly increased, and the levels of SOD, CAT, GSH-Px and GSH were significantly decreased. This result suggested the presence of oxidative damage in kidney tissues of DM rats. DN involves multiple pathologies, including abnormal glucose metabolism, oxidative stress, endoplasmic reticulum stress and inflammatory responses. Novel therapeutic treatments, in addition to identifying cellular processes underlying the pathogenesis of DN, may establish future successful treatments for DN.

Autophagy is a process that involves the removal of damaged proteins and organelles to maintain cellular homeostasis under various stress conditions and includes macroautophagy, microautophagy and chaperone-mediated autophagy (30). Autophagy can regulate a variety of stress responses, and disruptions in this regulatory mechanism may be related to age and the pathogenesis of DM-related diseases (31,32). It has previously been reported that in STZ-induced type 1 DM or HG conditions, the autophagic activity of podocytes is reduced, accompanied by a decrease in expression levels of autophagy-related proteins, Beclin-1, ATG12-5 and LC3 (33,34). Li and Siragy (35) also reported defective autophagy, and decreased LC3II and P62 accumulation in podocytes cultured with HG, suggesting that hyperglycemia reduces autophagic activity in podocytes. However, in other previous studies, the expression of the autophagy-related proteins LC3II and Beclin-1, and the number of autophagosomes, were found to increase in podocytes during HG treatment (36,37). This is consistent with studies conducted by Lenoir *et al* (38) and Dong *et al* (39), which reported similar results in primary podocytes and podocyte cell lines, suggesting that HG promotes autophagy in podocytes. Katsuragi *et al* (40) reported that the protein expression levels of LC3II and P62 were significantly increased in HK-2 cells after exposure to late glycosylation end products, suggesting that the accumulation of autophagosomes is caused by reduced lysosomal degradation in renal tubules. In the present study, it was demonstrated that the expression levels of LC3II and P62 were significantly increased in the kidney tissue of DM rats. In the late stage of DM, glucose utilization is deficient and other substrates used for energy are used preferentially, which can result in nutritional deficiencies. In this situation, LC3I is rapidly converted to LC3II, which results in the formation of autophagosomes to degrade proteins and damaged organelles to provide energy (41). P62 is a multifunctional protein that can link ubiquitinated proteins to LC3/ATG8 separately and undergoes self-oligomerization, entering the autophagolysosome to degrade ubiquitinated substrates (42). However, when the expression of P62 is upregulated, the degradation of autophagic lysosomes is impaired, resulting in poor autophagic flux and the accumulation of large amounts of autophagosomes, which may also be a potential reason for the occurrence of ESRD. In the present study, it was further demonstrated that HG prevented the degradation of autophagic lysosomes in NRK-52E cells as P62 was increased, which inhibited the autophagic flux.

AMPK is a key enzyme in the protein kinase signaling transduction chain and is also an important regulator of intracellular energy and metabolic balance (43). Activation of AMPK promotes the early inhibition of mTOR and induces autophagy (44). However, in the present study, AMPK phosphorylation was inhibited in the kidneys of DM rats and the protein expression levels of P62 were increased, demonstrating inhibition of the autophagic flux in DN, which could lead to kidney injury. AMPK can also phosphorylate the Raptor subunit of the mTOR complex 1 (mTORC1), which inhibits activation of mTORC1 (45). In the present study, it was demonstrated that phosphorylation of PI3K/AKT/mTOR was increased in the kidneys of DM rats and NRK-52E cells, which further suggested that HG prevented the autophagic flux. Therefore, renal injury could be prevented by promoting autophagy degradation.

MLT is an indoleamine that is synthesized by the pineal gland and produced by peripheral organs, such as the retina, Harderian glands, intestines and skin (46). The secretion of MLT follows a circadian rhythm, which is suppressed during the day and active at night (47,48). Therefore, in the present study, MLT treatment was administered in the night. MLT has numerous biological activities, including antioxidant, anti-inflammatory and anti-apoptotic properties, and the mechanisms by which MLT protects against DN include the regulation of ROS and AMPK signaling (49). In the present study, it was demonstrated that oxidative damage, mitochondrial damage and fibrosis in renal tissue was alleviated in DM rats after receiving MLT treatment. Meanwhile, the expression levels of LC3II and P62 were downregulated *in vitro* and *in vivo*. These findings indicated that MLT promoted autophagy degradation, which facilitated the occurrence of autophagy. Previous studies also indicated that MLT inhibits cell death by mediating autophagy (50,51). In addition, MLT also inhibited the phosphorylation of PI3K/AKT/mTOR in the kidneys of DM rats and NRK-52E cells, which further demonstrated the protective

effect of MLT through the regulation of autophagy. A previous study reported that MLT can effectively alleviate nickel-induced brain injury by activating the PI3K/AKT/mTOR signaling pathway (52). In the present study, it was also demonstrated that MLT treatment promoted the protein expression levels of MT1 and MT2 *in vivo* and *in vitro*, which may be beneficial to renal injury. In a previous study, MLT inhibited apoptosis by binding to surface membrane receptors MT1 and MT2 in chondrocytes (53), which further indicated the importance of MT1 and MT2 in renal injury. Taken together, these data suggested that MLT may serve a role in protecting against renal injury in DM and NRK-52E cell injury by alleviating the impairment of autophagy, promoting the degradation of misfolded proteins and damaged organelles, and attenuating renal fibrosis.

In conclusion, MLT exerts a protective effect against renal injury in DM rats and NRK-52E cells by alleviating the impairment of autophagy (Fig. 6). The present study provided novel evidence for the relationship between MLT and autophagy in the context of HG treatment. MLT promoted autophagy degradation by regulating the autophagic flux, which further alleviated kidney damage. In future studies, specific components of the AMPK/PI3K/AKT/mTOR signaling pathway and the process of autophagy should be investigated to further confirm the conclusions reached in the present study.

Acknowledgements

Professor Lin Wang (Shandong Agricultural University, College of Veterinary Medicine, Taian, Shangdong, China) provided the GFP-RFP-LC3 plasmid.

Funding

This work was supported by the Priority Academic Program Development of Jiangsu Higher Education Institutions.

Availability of data and materials

The datasets used and/or analyzed during the current study are available from the corresponding author on reasonable request.

Authors' contributions

ZL and YL conceived and designed the study. NL performed the experiment, figure preparation and manuscript draft. NL and YM developed the methods and performed data analysis. NL and YW acquired and interpreted the data. NL wrote and revised the paper. ZL and YL confirm the authenticity of all the raw data. All authors agree to be accountable for all aspects of the work in ensuring that questions related to the accuracy or integrity of any part of the work are appropriately investigated and resolved. All authors have read and approved the final manuscript.

Ethics approval and consent to participate

The experimental procedures were approved by the Ethics Committee of Yangzhou University [Yangzhou, China; approval no. SYXK (Su) 2022-0044].

Patient consent for publication

Not applicable.

Competing interests

The authors declare that they have no competing interests.

References

1. Sha J, Sui B, Su X, Meng Q and Zhang C: Alteration of oxidative stress and inflammatory cytokines induces apoptosis in diabetic nephropathy. Mol Med Rep 16: 7715-7723, 2017.
2. Thibodeau JF, Holterman CE, Burger D, Read NC, Reudelhuber TL and Kennedy CR: A novel mouse model of advanced diabetic kidney disease. PLoS One 9: e113459, 2014.
3. Gao Y, Ma Y, Xie D and Jiang H: ManNAc protects against podocyte pyroptosis via inhibiting mitochondrial damage and ROS/NLRP3 signaling pathway in diabetic kidney injury model. Int Immunopharmacol 107: 108711, 2022.
4. Zhong Y, Liu J, Sun D, Guo T, Yao Y, Xia X, Shi C and Peng X: Dioscin relieves diabetic nephropathy via suppressing oxidative stress and apoptosis, and improving mitochondrial quality and quantity control. Food Funct 13: 3660-3673, 2022.
5. Teh YM, Mualif SA and Lim SK: A comprehensive insight into autophagy and its potential signaling pathways as a therapeutic target in podocyte injury. Int J Biochem Cell Biol 143: 106153, 2022.
6. Medras ZJH, Mostafa YM, Ahmed AAM and EI-Sayed NM: Arctigenin improves neuropathy via ameliorating apoptosis and modulating autophagy in streptozotocin-induced diabetic mice. CNS Neurosci Ther: May 11, 2023 (Epub ahead of print).
7. Wang LH, Wang YY, Liu L and Gong Q: From diabetes to diabetic complications: Role of autophagy. Curr Med Sci 43: 434-444, 2023.
8. Liu L, Dai WZ, Zhu XC and Ma T: A review of autophagy mechanism of statins in the potential therapy of Alzheimer's disease. J Integr Neurosci 21: 46, 2022.
9. Feng H, Wang N, Zhang N and Liao HH: Alternative autophagy: Mechanisms and roles in different diseases. Cell Commun Signal 20: 43, 2022.
10. Lim JH, Kim HW, Kim MY, Kim TW, Kim EN, Kim Y, Chung S, Kim YS, Choi BS, Kim YS, *et al*: Cinacalcet-mediated activation of the CaMKKβ-LKB1-AMPK pathway attenuates diabetic nephropathy in db/db mice by modulation of apoptosis and autophagy. Cell Death Dis 9: 270, 2018.
11. Song FQ, Song M, Ma WX, Gao Z, Ti Y, Zhang X, Hu BA, Zhong M, Zhang W and Yu Y: Overexpressing STAMP2 attenuates diabetic renal injuries via upregulating autophagy in diabetic rats. Biochem Biophys Res Commun 579: 47-53, 2021.
12. Lian CY, Chu BI, Xia WH, Wang ZY, Fan RF and Wang L: Persistent activation of Nrf2 in a p62-dependent non-canonical manner aggravates lead-induced kidney injury by promoting apoptosis and inhibiting autophagy. J Adv Res 46: 87-100, 2023.
13. Hsiao CC, Lin CC, Hou YS, Ko JY and Wang CJ: Low-energy extracorporeal shock wave ameliorates streptozotocin induced diabetes and promotes pancreatic beta cells regeneration in a rat model. Int J Mol Sci 20: 4934, 2019.
14. Owino S, Contreras-Alcantara S, Baba K and Tosini G: Melatonin signaling controls the daily rhythm in blood glucose levels independent of peripheral clocks. PLoS One 11: e0148214, 2016.
15. Agil A, Chayah M, Visiedo L, Navarro-Alarcon M, Rodríguez Ferrer JM, Tassi M, Reiter RJ and Fernández-Vázquez G: Melatonin improves mitochondrial dynamics and function in the kidney of Zücker diabetic fatty rats. J Clin Med 9: 2916, 2020.
16. Yapislar H, Haciosmanoglu E, Sarioglu T and Ekmekcioglu C: The melatonin MT_2 receptor is involved in the anti-apoptotic effects of melatonin in rats with type 2 diabetes mellitus. Tissue Cell 76: 101763, 2022.
17. Wang W, Zhang J, Wang X, Wang H, Ren Q and Li Y: Effects of melatonin on diabetic nephropathy rats via Wnt/β-catenin signaling pathway and TGF-β-Smad signaling pathway. Int J Clin Exp Pathol 11: 2488-2496, 2018.
18. Fan Z, Qi X, Yang W and Wu Y: Melatonin ameliorates renal fibrosis through the inhibition of NF-κB and TGF-β1/Smad3 pathways in db/db diabetic mice. Arch Med Res 51: 524-534, 2020.

19. Wei J, Wang Y, Qi X, Fan Z and Wu Y: Melatonin ameliorates hyperglycaemia-induced renal inflammation by inhibiting the activation of TLR4 and TGF-β1/Smad3 signalling pathway. Am J Transl Res 12: 1584-1599, 2020.
20. Chen YT, Yang CC, Sun CK, Chiang HJ, Chen YL, Sung PH, Zhen YY, Huang TH, Chang CL, Chen HH, *et al*: Extracorporeal shock wave therapy ameliorates cyclophosphamide-induced rat acute interstitial cystitis though inhibiting inflammation and oxidative stress-in vitro and in vivo experiment studies. Am J Transl Res 6: 631-648, 2014.
21. Xu Q and Cheung RTF: Melatonin mitigates type 1 diabetes-aggravated cerebral ischemia-reperfusion injury through anti-inflammatory and anti-apoptotic effects. Brain Behav: e3118, 2023 (Epub ahead of print).
22. Yu L, Gong B, Duan W, Fan C, Zhang J, Li Z, Xue X, Xu Y, Meng D, Li B, *et al*: Melatonin ameliorates myocardial ischemia/reperfusion injury in type 1 diabetic rats by preserving mitochondrial function: Role of AMPK-PGC-1α-SIRT3 signaling. Sci Rep 7: 41337, 2017.
23. Zhang Y, Wang Y, Xu J, Tian F, Hu S, Chen Y and Fu Z: Melatonin attenuates myocardial ischemia-reperfusion injury via improving mitochondrial fusion/mitophagy and activating the AMPK-OPA1 signaling pathways. J Pineal Res 66: e12542, 2019.
24. Siddhi J, Sherkhane B, Kalavala AK, Arruri V, Velayutham R and Kumar A: Melatonin prevents diabetes-induced nephropathy by modulating the AMPK/SIRT1 axis: Focus on autophagy and mitochondrial dysfunction. Cell Biol Int 46: 2142-2157, 2022.
25. Qiu WH, An S, Wang T, Li J, Yu B, Zeng Z, Chen Z, Lin B, Lin X and Gao YG: Melatonin suppresses ferroptosis via activation of the Nrf2/HO-1 signaling pathway in the mouse model of sepsis-induced acute kidney injury. Int Immunopharmacol 112: 109162, 2022.
26. Morya AK, Ramesh PV, Kaur K, Gurnani B, Heda A, Bhatia K and Sinha A: Diabetes more than retinopathy, it's effect on the anterior segment of eye. World J Clin Cases 11: 3736-3749, 2023.
27. Cooper ME: Pathogenesis, prevention, and treatment of diabetic nephropathy. Lancet 352: 213-219, 1998.
28. Lu Q, Ji XJ, Zhou YX, Yao XQ, Liu YQ and Yin XX: Quercetin inhibits the mTORC1/p70S6K signaling-mediated renal tubular epithelial-mesenchymal transition and renal fibrosis in diabetic nephropathy. Pharmacol Res 99: 237-247, 2015.
29. Kashihara N, Haruna Y, Kondeti VK and Kanwar YS: Oxidative stress in diabetic nephropathy. Curr Med Chem 17: 4256-4269, 2010.
30. Ichimiya T, Yamakawa T, Hirano T, Yokoyama Y, Hayashi Y, Hirayama D, Wagatsuma K, Itoi T and Nakase H: Autophagy and autophagy-related diseases: A review. Int J Mol Sci 21: 8974, 2020.
31. Gonzalez CD, Lee MS, Marchetti P, Pietropaolo M, Towns R, Vaccaro MI, Watada H and Wiley JW: The emerging role of autophagy in the pathophysiology of diabetes mellitus. Autophagy 7: 2-11, 2011.
32. Rubinsztein DC, Mariño G and Kroemer G: Autophagy and aging. Cell 146: 682-695, 2011.
33. Ding DF, You N, Wu XM, Xu JR, Hu AP, Ye XL, Zhu Q, Jiang XQ, Miao H, Liu C and Lu YB: Resveratrol attenuates renal hypertrophy in early-stage diabetes by activating AMPK. Am J Nephrol 31: 363-374, 2010.
34. Xu XH, Ding DF, Yong HJ, Dong CL, You N, Ye XL, Pan ML, Ma JH, You Q and Lu YB: Resveratrol transcriptionally regulates miRNA-18a-5p expression ameliorating diabetic nephropathy via increasing autophagy. Eur Rev Med Pharmacol Sci 21: 4952-4965, 2017.
35. Li C and Siragy HM: (Pro)renin receptor regulates autophagy and apoptosis in podocytes exposed to high glucose. Am J Physiol Endocrinol Metab 309: E302-E310, 2015.
36. Ma T, Zhu J, Chen X, Zha D, Singhal PC and Ding G: High glucose induces autophagy in podocytes. Exp Cell Res 319: 779-789, 2013.
37. Wei M, Li Z and Yang Z: Crosstalk between protective autophagy and NF-κB signal in high glucose-induced podocytes. Mol Cell Biochem 394: 261-273, 2014.
38. Lenoir O, Jasiek M, Hénique C, Guyonnet L, Hartleben B, Bork T, Chipont A, Flosseau K, Bensaada I, Schmitt A, *et al*: Endothelial cell and podocyte autophagy synergistically protect from diabetes-induced glomerulosclerosis. Autophagy 11: 1130-1145, 2015.
39. Dong C, Zheng H, Huang S, You N, Xu J, Ye X, Zhu Q, Feng Y, You Q, Miao H, *et al*: Heme oxygenase-1 enhances autophagy in podocytes as a protective mechanism against high glucose-induced apoptosis. Exp Cell Res 337: 146-159, 2015.
40. Katsuragi Y, Ichimura Y and Komatsu M: p62/SQSTM1 functions as a signaling hub and an autophagy adaptor. FEBS J 282: 4672-4678, 2015.
41. Han YP, Liu LJ, Yan JL, Chen MY, Meng XF, Zhou XR and Qian LB: Autophagy and its therapeutic potential in diabetic nephropathy. Front Endocrinol (Lausanne) 14: 1139444, 2023.
42. Komatsu M, Kageyama S and Ichimura Y: p62/SQSTM1/A170: Physiology and pathology. Pharmacol Res 66: 457-462, 2012.
43. Herzig S and Shaw RJ: AMPK: Guardian of metabolism and mitochondrial homeostasis. Nat Rev Mol Cell Biol 19: 121-135, 2018.
44. Kma L and Baruah TJ: The interplay of ROS and the PI3K/Akt pathway in autophagy regulation. Biotechnol Appl Biochem 69: 248-264, 2022.
45. Gwinn DM, Shackelford DB, Egan DF, Mihaylova MM, Mery A, Vasquez DS, Turk BE and Shaw RJ: AMPK phosphorylation of raptor mediates a metabolic checkpoint. Mol Cell 30: 214-226, 2008.
46. Tan DX, Hardeland R, Back K, Manchester LC, Alatorre-Jimenez MA and Reiter RJ: On the significance of an alternate pathway of melatonin synthesis via 5-methoxytryptamine: Comparisons across species. J Pineal Res 61: 27-40, 2016.
47. Linowiecka K, Slominski AT, Reiter RJ, Böhm M, Steinbrink K, Paus R and Kleszczyński K: Moletanin: A potential regulator of DNA methylation. Antioxidants (Basel) 12: 1155, 2023.
48. Shao R, Wang Y, He C and Chen L: Melatonin and its emerging physiological role in reproduction: A review and update. Curr Mol Med: Apr 17, 2023 (Epub ahead of print).
49. Zhang H, Zhang HM, Wu LP, Tan DX, Kamat A, Li YQ, Katz MS, Abboud HE, Reiter RJ and Zhang BX: Impaired mitochondrial complex III and melatonin responsive reactive oxygen species generation in kidney mitochondria of db/db mice. J Pineal Res 51: 338-344, 2011.
50. Dun RL, Lan TY, Tsai J, Mao JM, Shao YQ, Hu XH, Zhu WJ, Qi GC and Peng Y: Protective effect of melatonin for renal ischemia-reperfusion injury: A systematic review and meta-analysis. Front Physiol 12: 791036, 2022.
51. Song D, Liu Y, Yao Y, Liu F, Tao W, Zhou X, Li R, Zhang X and Li X: Melatonin improves bisphenol A-induced cell apoptosis, oxidative stress and autophagy impairment via inhibition of the p38 MAPK signaling pathway in FLK-BLV cells. Environ Toxicol 37: 1551-1562, 2022.
52. Qiao S, Sun Y, Jiang Y, Chen X, Cai J, Liu Q and Zhang Z: Melatonin ameliorates nickel induced autophagy in mouse brain: Diminution of oxidative stress. Toxicology 473: 153207, 2022.
53. Lim HD, Kim YS, Ko SH, Yoon IJ, Cho SG, Chun YH, Choi BJ and Kim EC: Cytoprotective and anti-inflammatory effects of melatonin in hydrogen peroxide-stimulated CHON-001 human chondrocyte cell line and rabbit model of osteoarthritis via the SIRT1 pathway. J Pineal Res 53: 225-237, 2012.